CoA Memo. No. 182

THE COLLEGE OF AERONAUTICS

AN INVESTIGATION INTO THE BASIC MECHANICS OF ORTHOGONAL MACHINING

- by -

H. Enahoro*

*Department of Production Engineering, The College of Aeronautics, Cranfield, Bedford.

(This report is based on a research project sponsored by the Science Research Council from 1963 to 1966).

C O N T E N T S

Section	Title	Page
	Summary	i
1.00	Introduction	1
1.01	The Rigid-plastic Solution	1
1.02	The Shear Zone Theory	2
2.00	Experimental Results	3
2.01	Hounsfield Tensometer	3
2.02	Loewe Milling Machine	4
2.03	Planing Machine	4
2.04	Plotting of Films	4
2.05	The Tool Dynamometer	5
2.06	Filming Procedure	5
3.00	Results	
3.01	Variation of Cutting Forces	7
3.02	Variation of Contact Length	7
3.03	Variation of Radius of Curvature	7
3.04	Variation of Cutting Ratio	7
3.05	Variation of Shear Zone Length	7
3.06	Effect of Tool Dig-in	8
3.07	Effect of Chip Curling Over	8
4.00	Discussion	9
	References	9

SUMMARY

Three machines were modified to enable orthogonal cuts to be taken over a speed range of 0.04 in per min to 50 ft per min. The very low speed films were used to verify an analytical solution to the cutting operation at the tool point. Over the whole range the results showed some agreement with other research results.

1.00 Introduction

Any analysis of orthogonal plane-strain cutting involves the following factors:

1. Idealisation of material
2. Friction
3. Rake angle

If the material is taken to be of the simplest kind, i.e. an ideal rigid-plastic material, we cannot reach any explanation of many well-known features of metal cutting such as effect of speed and depth of cut, for these effects do not enter into the solution of the elementary problem. This has lead to confusion in the past, and to dismissal of simple solutions as being unavailing. However, it should not be concluded that the simple solutions are wrong, and it is a matter of regret that no one has taken the trouble to control experimental conditions so as to obtain confirmation. Such work may not go far towards elucidating the mechanics of cutting under workshop conditions but it is a good precept to tackle the simplest problems first. While the work proposed here could be treated as an investigation complete within itself, it is hoped that it will help towards clarifying the action of tools as they are at present conceived.

1.01 The Rigid-Plastic Solution: A rigid-plastic material means one which flows at a constant yield stress k whenever the maximum shear stress at any point reaches this value, and yet undergoes no deformation at all while the shear stress is less than this value. The stress-strain diagram is shown in Fig. 1(a). In this material a discontinuous change in shear strain may occur across a single line. This is not possible for the strain-hardening material illustrated in Fig. 1(b) for shear stresses on either side of such a line would not be in static equilibrium. Therefore, with a rigid-plastic material, it is assumed that all the shear strain in the chip is acquired as a particle crosses a single line AB, as shown in Fig. 2, and that no deformation occurs in material on either side of this line. Although such a line is often referred to as a slip line, the term is misleading, as no slip occurs. Let the tool be stationary with the material advancing at speed V while the chip travels up the tool face at speed V. The rake angle is α and the slip line is inclined to the horizontal at anyle ϕ. The depth of cut is t and the chip thickness is T. As the deformation occurs at constant volume, velocity components normal to AB are equal on either side of the line, giving

$$\frac{v}{V} = \frac{t}{T} = \frac{\sin\phi}{\cos(\phi-\alpha)} \qquad (1)$$

Incidentally, this equation allows us to calculate ϕ from the ratio of chip length to length of cut, this ration being equal to the ratio t/T. Shear strain is equal to relative tangential velocity of particles on either side of the slip line divided by the normal component of velocity,

$$\gamma = \cot \phi + \tan (\phi - \alpha) \qquad (2)$$

As friction is assumed absent, the work done by the tool can be equated to work absorbed by the material to give the cutting force per unit width of cut,

$$F = k\gamma t \qquad (3)$$

As the slip line AB is straight, the pressure p acting normal to AB is the same at all points along this line. The tool force must act normal to the frictionless tool surface, so the triangle of forces for the chip gives

$$p = k \tan (\phi - \alpha) \qquad (4)$$

Evaluating the resultant cutting force F from normal and tangential stresses along AB and inserting it in equation (3) gives shear strain as in equation (2), showing that the equations are compatible.

1.02 The Shear Zone Theory

There is substantial experimental evidence from direct observation of chip formation to show that during cutting deformation does not take place on a single shear plane but over a finite zone.

Further experimental evidence, (1), suggests that cutting takes place over a plastic zone of the shape shown in Fig. 3. One of the assumptions made in the shear plane type of analysis is that the work material is an ideal plastic-rigid material, that is, the shear flow stress of the material is assumed constant.

In a detailed analysis of an experimentally observed shear zone it was found that neither the shape of the shear zone nor the position of the resultant cutting force were consistent with the concept of an ideal plastic-rigid material and could only be explained if the shear flow stress of the work material was considered to vary.

Implicit in all shear plane solutions is that the normal (hydrostatic) stress is constant along the length of the shear plane. That this is not so for a material having a variable flow stress can be seen by considering an element of a shear zone lying between two adjacent slip lines. As the material passes through the shear zone its flow stress will alter as a result of work-hardening, temperature, strain rate, etc.

In recent papers it has been suggested that over part of the tool-chip contact zone the chip does not slide but sticks to the tool, chip flow taking place by shear within the body of the chip. Sticking contact is inconsistent with steady state cutting and a slip-line field model of chip flow is presented, (2), which does not include sticking contact and which is consistent with the relevant experimental observations.

2.0 EXPERIMENTAL PROCEDURE

Over 600 tests were carried out covering the following range of cutting conditions:

Work Materials	:	Pure Copper, Aluminium Alloy, Mild Steel.
Tool Material	:	High Speed Steel
Cutting Speeds	:	0.04, 0.2, 1.0, 5.0 in. per min. 2.0, 10, 50 ft per min.
Depths of Cut	:	0.001″ to 0.008″ at increments of 0.001″ or 0.002″
Rake Angles	:	20°, 25°, 30°, 35°, 40°, 45°
Tests Machines	:	Hounsfield Tensometer (0.04 and 0.2 in per min) Horizontal Miller (1.0 and 5.0 in per min) Planer (2, 10 and 50 ft per min)
Force-measuring Instrument	:	Sigma Dynamometer with U.V. Recorder
Cameras	:	Cine Kodak Special, 16 mm (8 - 64 frames per sec) Wollensak Fastax, 16 mm (8000 frames per sec max)
Projector	:	Specto Analyser fitted with remote control mechanism.

The three machines used for the tests were modified to convert them into planing machines operating at various ranges of speeds to cover the overall range of 0.04 in per min to 50 ft per min. The modification of the Hounsfield Tensometer was designed to give cutting speeds corresponding to strain rate equivalent to standard materials-testing rates. It would thus be possible to compare results from metal cutting and compression tests carried out at strain rates of the same order of magnitude. The upper limit of 50 ft per min on the planer was fixed by the length of the specimen and the camera speed because the cutting speed is magnified by as many times as the magnification of the lens.

The specimens were polished and etched with the appropriate etching agents to show the grain structure which was used as a grid to trace the flow pattern during each cut. The forces were recorded when steady state had been achieved; in some cases of short duration, the forces were recorded over the whole length of cut so as to investigate the build up to steady state and the amount of overshoot due to tool dig-in and the decay at the end of the cut. Film records were taken at suitable frame speeds while the forces were being recorded. The films were processed and are at present being analysed.

2.01 Hounsfield Tensometer

0.04 in. to 1 in. per min.: A Hounsfield Tensometer was modified into a cutting test machine to cover this range and is shown on Plate 2. The machine was supported on the table of a planer. The slide carrying the specimen was driven by the tensometer leadscrew which was in turn driven by an electric motor through a pulley system. The cutting tool was held in a Sigma dynamometer and forces were recorded on an Ultra Violet Recorder. Films were taken through a microscope by a Cine Kodak Special camera and microscope objectives and eyepieces gave object-to-film magnification ranging from 6 to 180 of the zone of operation.

The former magnification is that usually encountered in the literature. The latter is limited by the field of view that can be accommodated on a 16 mm film. Higher magnification results in the tool point alone occupying almost the whole frame to the exclusion of the chip. A projected image 3 ft wide on a screen thus corresponds to magnification of about 330 to 10,000 for the object-to-film magnification of 6 to 180 respectively.

2.02 Loewe Milling Machine

0.5 in to 6 in per min.: This range was covered by the Loewe milling machine which is shown in the modified form on Plate 3. Though the miller will cut at a higher speed, the Cine Kodak camera, with its maximum speed of 64 frames per second, would tend to show blurred images if used at much higher speeds than 6 in. per minute. The cutting tool and force recording arrangement were as on the tensometer.

The modifications to the miller were as follows. The tool dynamometer was supported on a cast iron angle plate designed for rigidity and vibration absorption. The machine crosshead was fixed in position and supported vertical and horizontal slides. This slide assembly carried a platform and enabled the microscope and camera supported on the platform to be focussed on the area of deformation.

2.03 Planing Machine

The higher range of cutting speeds, from 6 in. per minute upwards, was covered by the planing machine shown on Plate 5. The photography was carried out with a Wollensak Fastex camera with a working range of 500 to 8,000 frames per second. The lower speeds operate through a D.C. circuit while the higher speeds require A.C. supply. The light source at these high filming speeds needs to be intense; for this purpose a stroboscopic lighting attachment was used.

2.04 Plotting of Films

Analysis of the films involves projecting them with a Spectro Analyser on to a sheet of paper on a projection board and tracing out the paths of individual grains to show the flow pattern from the workpiece into the chip. It is possible from the plots to determine accurately the magnification, length of cut, chip thickness, chip ratio, length, width, area and length to width ratio of the shear zone, shear angle, radius of curvature of the chip and chip-tool contact length and hence to evaluate such parameters as the friction coefficient, friction angle, friction force, shear stress, shear force and resultant cutting force. From the force traces it is possible to determine the steady state forces, the amount of force overshoot corresponding to the dig-in of the tool before the cut steadies the exact length of time a cut of the same depth takes for the same machine speed setting under different conditions of work material and rake angle.

Before the remote controlled projector became available, plotting of the films required two people, one of whom operated the projector. There was some difficulty at the time in obtaining help; this, allied with the fact that the original projector was frequently developing a fault, resulted in the purchase of the projector with the remote control enabling only one operator to do the plotting. The projector, however, goes out of focus so often that the single operator has to go and refocus every few minutes; it therefore takes one operator with a remote control projector much more time to do the same amount of work as two operators with a manually controlled projector. Specto have been approached about this problem but consider the behaviour of the instrument to be within acceptable limits. For this type of work, however, the operator needs to keep his eyes fixed on one small point among several other adjacent similar points; these merge into each other when the image goes out of focus and the point being traced is sometimes lost in walking away to refocus the instrument.

2.05 The Tool Dynamometer: The instrument was a Sigma three-component force measuring dynamometer working on the principle of a gap galvanometer. The tool was held in a diaphragm at the front; this diaphragm at the front; this diaphragm was bolted on to a light lever carrying a plate at the rear. This plate moved in and out of grooves at its edges thereby decreasing or increasing the gap when the diaphragm in front was deflected.

The resulting signal was amplified through a minirack and metered on an Ultraviolet Recorder. The calibration chart is shown in Fig. 3; calibration of the instrument was checked periodically during the course of the project.

2.06 Filming Procedure: When a moving object is filmed through a microscope, the camera sees it moving as many times as fast as the object is magnified. The conventional laboratory camera with a maximum speed of 64 frames per sec can resolve objects moving at about 24 in per min without 'blurring' the image. If such a camera is used to film through a microscope that magnifies about 6 times then the maximum cutting speed must be about 4 in per min. A magnification of 6 is, however, not enough to permit sufficiently close observation of the shear zone. A magnification of 60 or above is necessary for this but whis would convert a cutting speed of even 0.5 in per min, the minimum on a milling machine, to 30 in per min. at the camera, which is too high. Thus the modification of the tensometer to a cutting test machine with a minimum speed of 0.04 in per min. was very necessary and has helped to solve the problem. Another advantage of this very low speed is that it allows time for proper alignment of the faces of the tool and the specimen to get them both in simultaneous focus while a cut is in progress. At higher speeds, time and specimen length required would be too great.

Plates 6 and 7 show stills from films taken at an object-to-film magnification of 60; as seen on the print, the magnifications are 400 and 1200 respectively; the test conditions were: material: mild steel, rake angle: 35°, depth of cut: 0.003". The tools used were ordinary sharp tools and are seen rounded only because of the very high magnification.

The next stage of the programme will include obtaining cine film records of the flow in the main and secondary plastic zones for a very wide range of cutting conditions and for different work materials including different cold-worked conditions. These records of the flow were later analysed.

3.00 RESULTS

3.01 Variation of Forces with:

3.01(a) Depth of Cut, t: Figs. 5 to 25 show that the Resultant Cutting force increased linearly as depth of cut increases.

3.01(b) Rake Angle: Cutting force decreases as rake angle increases.

3.01(c) Cutting Speed: The behaviour of cutting force with respect to speed can only be seen from the derived curves in Figs. 26 to 28. All three curves for the different specimen materials exhibit much the same characteristics; starting at the lowest speed, the resultant cutting force first decreases then increases to a maximum and then falls again. At the highest speed the difference in the values for the different rake angles is small compared with values at other speeds.

3.01(d) Work Material: Fig. 29 shows that the cutting forces are highest for MS followed by Cu and finally Al. The comparison is for the same cutting conditions in speed and rake angle.

3.02 Variation of Contact Length with:

3.02(a) Depth of Cut: Fig. 30 shows that the contact length increases with depth of cut.

3.02(b) Rake Angle: The contact length decreases as rake angle increases.

3.03 Variation of Radius of Curvature with

3.03(a) Depth of Cut: Fig. 31 shows that the radius of curvature increases as depth of cut increases.

3.03(b) Rake Angle: The radius decreases as rake angle increases.

3.04 Variation of Cutting Ratio (and Shear Angle) with:

3.04(a) Depth of Cut: Fig. 32 shows that the cutting ratio (and hence the shear angle) decreases slightly as depth of cut increases.

3.04(b) Rake Angle: Cutting ratio increases as rake angle increases.

3.05 Variation of Shear Zone Length with:

3.05(a) Depth of Cut: Fig. 33 shows that the equivalent shear zone length increases with depth of cut.

3.05(b) Rake Angle: The length decreases as rake angle increases.

3.06 Effect of Tool Dig-in: At very large rake angles or with M.S. at most rake angles when cutting with a tool clamped in a dynamometer, the tool tends to dig-in at the start of the cut before it levels out to its steady-state reading. Fig. 34 shows four force traces for machining with 35° rake angle at 5.25 in per min at 0.002″ depth of cut.

(a) M.S.

(b) Cu

(c) Al

(d) Al (45° rake angle)

It can be seen that the M.S. force increases very sharply at the start; the height above the steady-state reading is called the overshoot and it increases with depth of cut. The length of overshoot is however almost independent of depth of cut.

The Cu trace is without any overshoot though it did appear once or twice; the build-up to the maximum value is more gradual than in the case of M.S.

The Aluminium alloy tends to machine with a built up edge. This shows quite clearly on the next trace. It must be stated, however, that the vertical scale is not the same for all four traces hence the Al-alloy appears to machine with higher forces than M.S. The irregular line for Al-alloy indicates that it is machining with built-up edges.

3.07 Effect of Chip Curling Over: Fig. 34(d) shows what happens when the chip curls over and touches the work material; the cutting force decreases. The vertical scale for (d) which shows a 0.007″ cut is different from that for (c) hence the characteristic trace for built up edge formation is not immediately obvious.

4.00 DISCUSSION

The modification of the Hounsfield Tensometer into a cutting test machine has made it easy to cut at such very low speeds that very highly magnified films of the cutting operation at the tool point is now possible; hence Plates 6 and 7. They showed that the naturally sharp tool really has a radius of the order of 0.0005" to 0.001". It was possible with the Hounsfield to attempt to verify the theoretical analysis in (2).

The graphs, Figs. 26 to 28, show an agreement with (3) that forces do not bear a linear relationship with speed. The range covered here is below the lowest speed used by the researchers whose worker's reported in (3) but seems to fit in well with the general behaviour of their curves.

Most of the conclusions that may be drawn from this work already appear in (2) and (4); this report is therefore a complement to these two papers, copies of which are enclosed.

REFERENCES

1. PALMER, W.B. and OXLEY, P.L.B.
'Mechanics of Orthogonal Machining'
Proc. I.M.E. 1959, Vol. 173, No. 24, p. 623.

2. ENAHORO, H. and OXLEY, P.L.B.
'Flow Along Tool-Chip Interface in Orthogonal Metal Cutting'
Jour. Mech. Eng. Sci., 1966, Vol. 8, No. 1, p. 36.

3. ZOREV, N.N.
'Metal Cutting Mechanics'
Pergammon Press, 1966.

4. ENAHORO, H. and WELSH, M.J.M.
'The Relevance of the Mechanics of Metal Cutting to Machinability'
ISI Special Report 94, 1967.

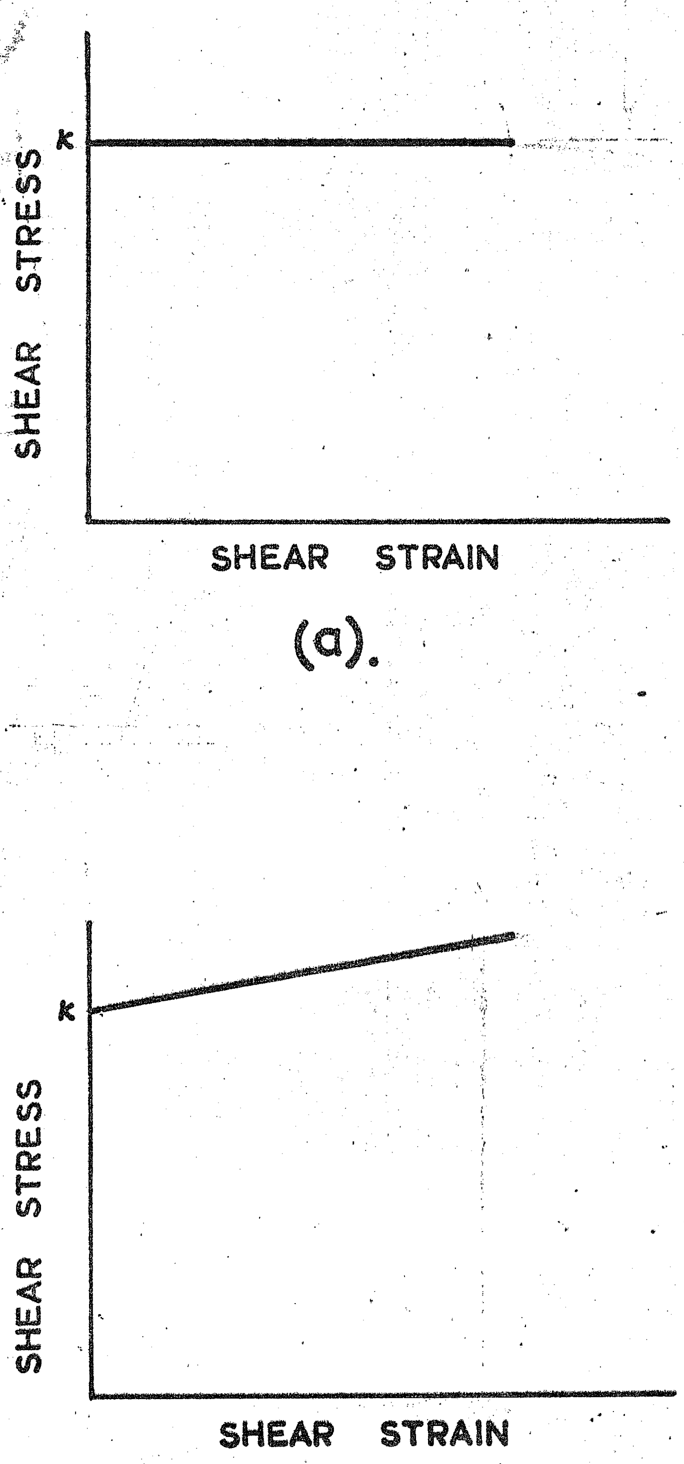

(a).

(b).

FIG. I

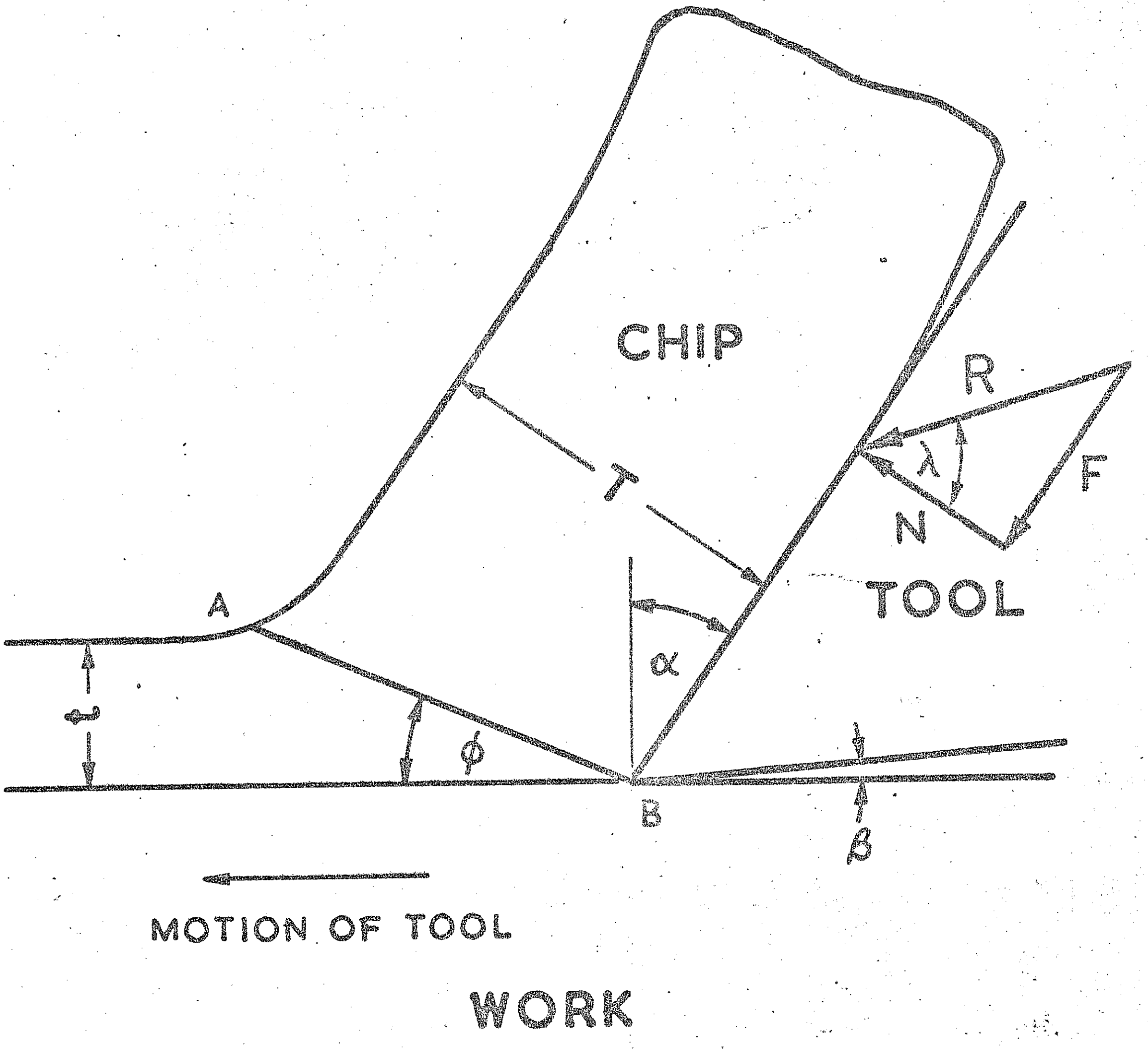

FIG. 2

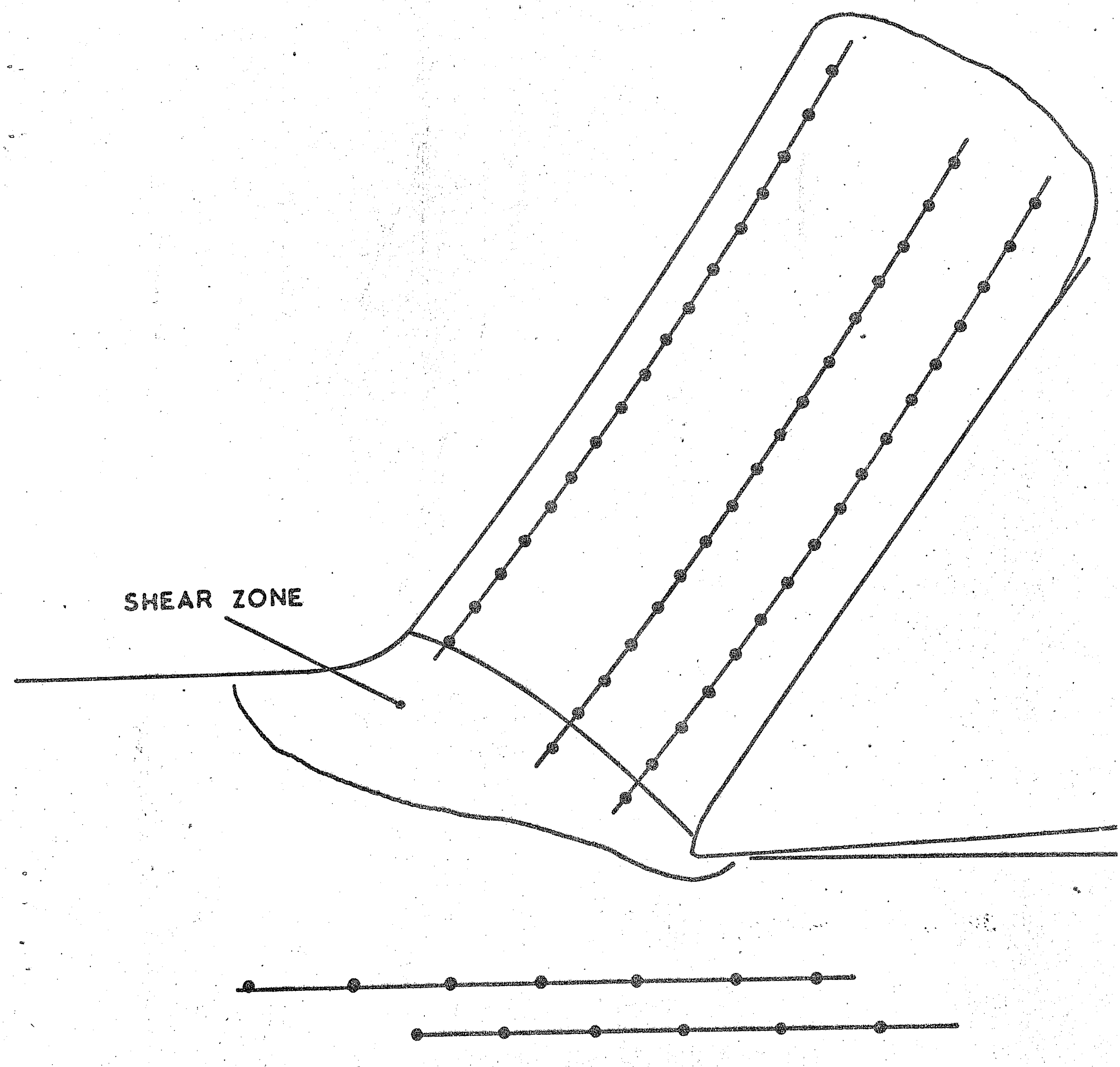

FIG. 3

FIG. 4

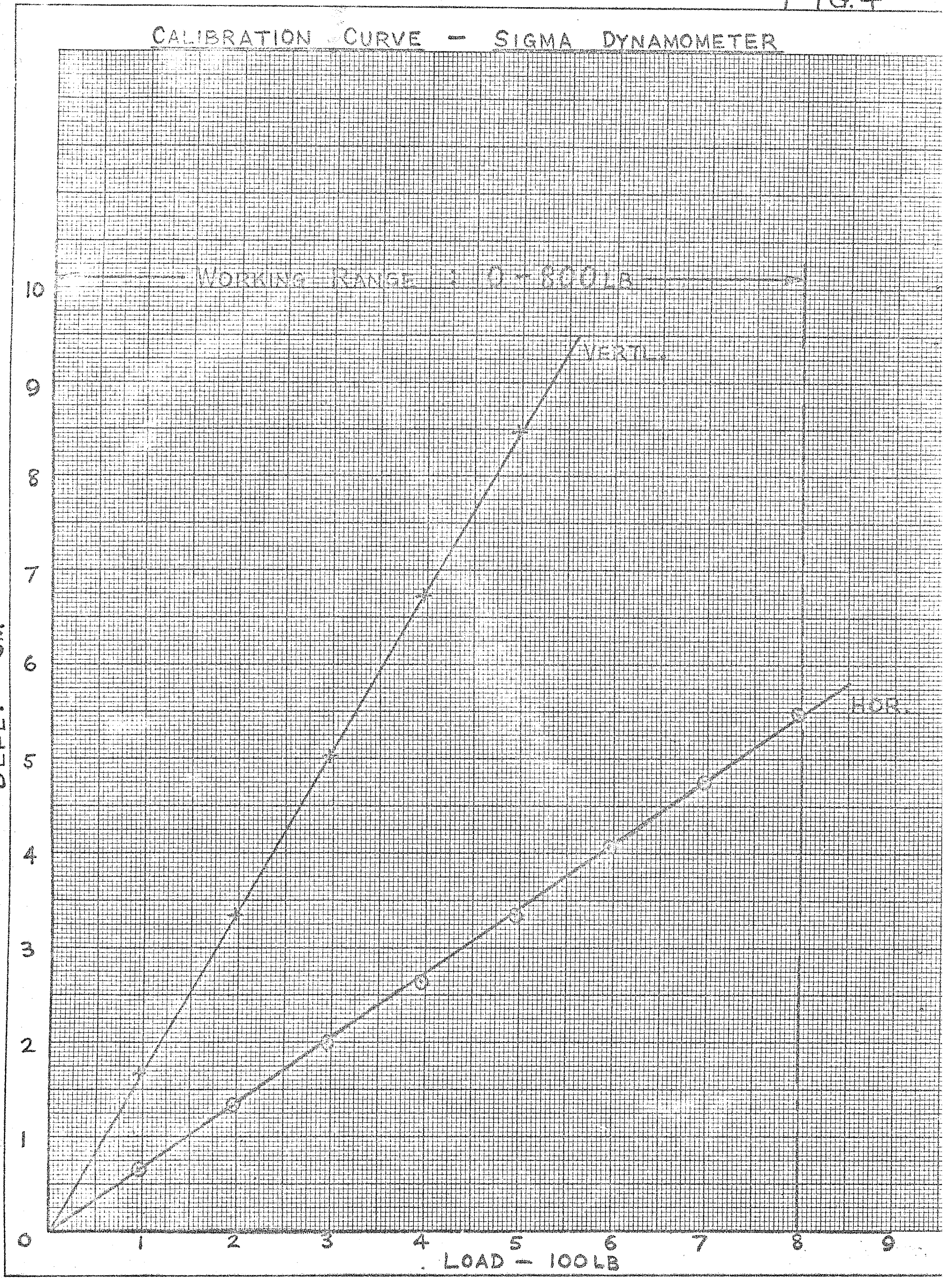
CALIBRATION CURVE - SIGMA DYNAMOMETER
WORKING RANGE : 0 - 800 LB
VERTL.
HOR.
DEFL. - CM
LOAD - 100 LB
0
1
2
3
4
5
6
7
8
9
10

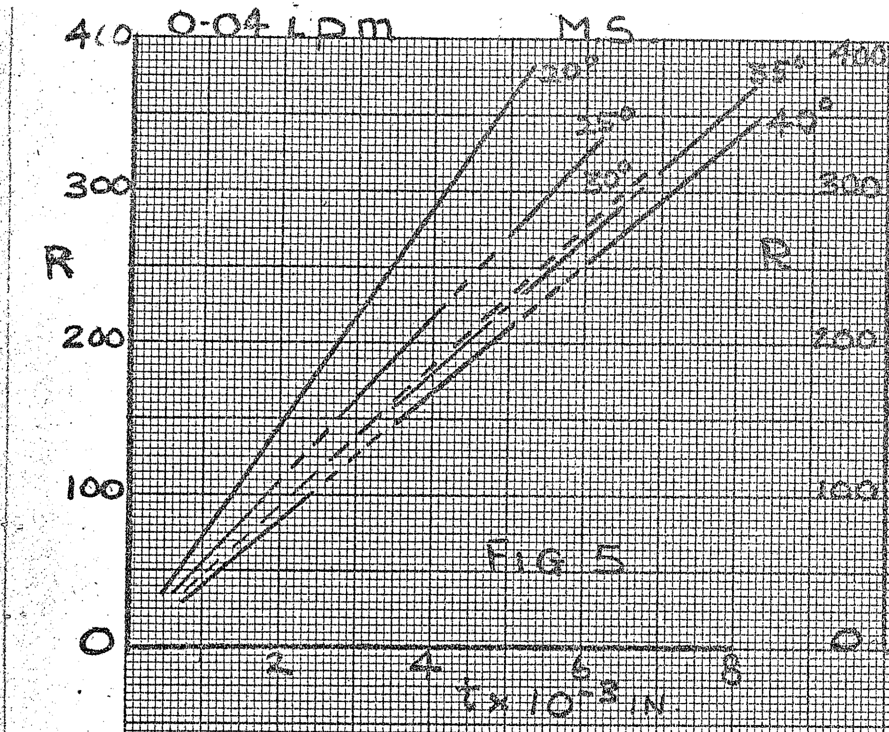
0·04 Lpm
M.S.
20°
25°
30°
35°
40°
R
Fig 5
t x 10-3 IN

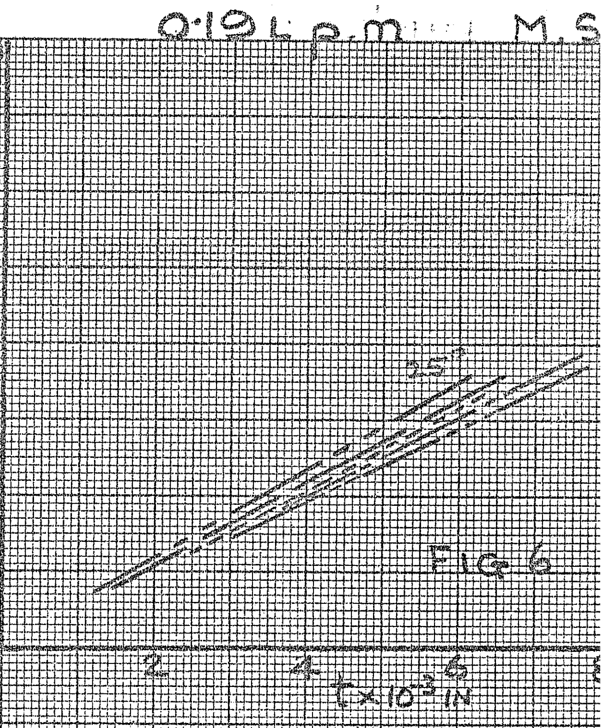
0·19 Lpm
M.S
R
25°
Fig 6
t x 10-3 IN

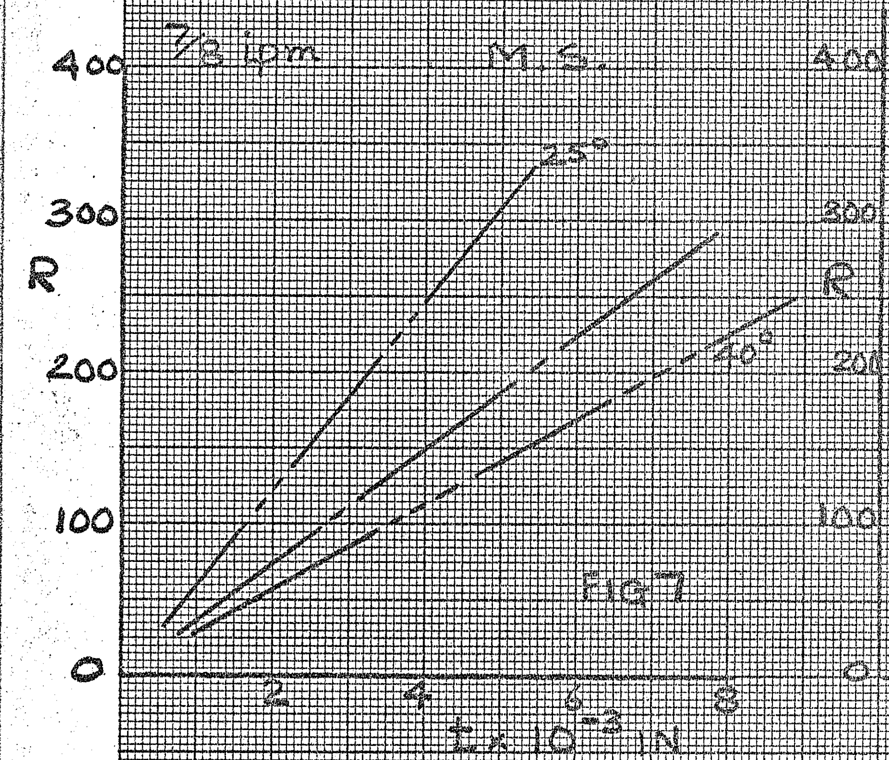
7/8 ipm
M.S.
R
25°
40°
Fig 7
t x 10-3 IN

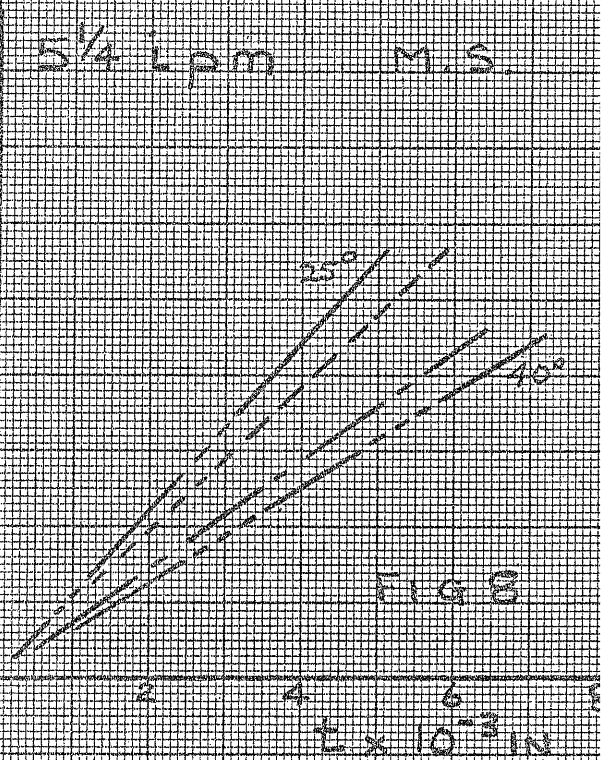
5¼ Lpm
M.S.
R
25°
40°
Fig 8
t x 10-3 IN

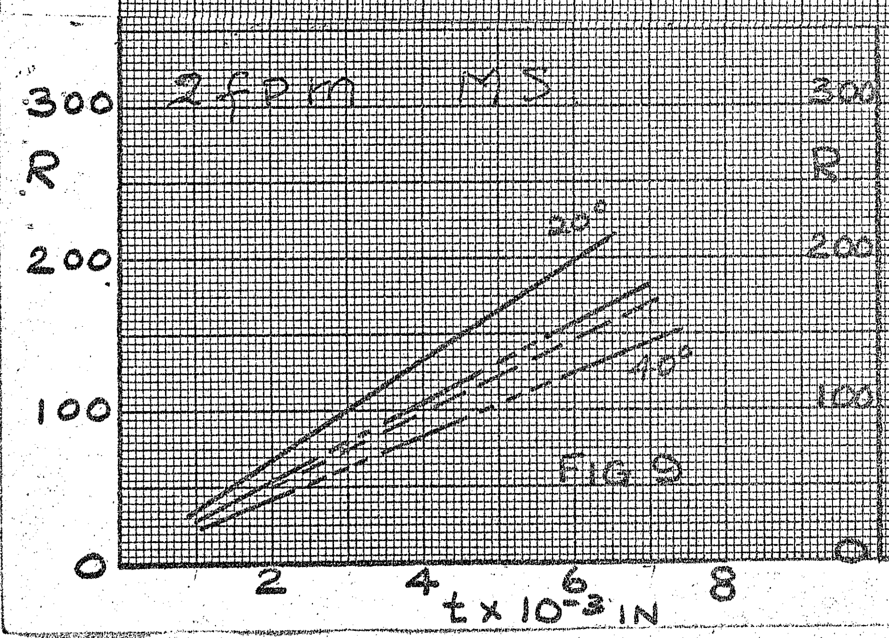
2 fpm
M S
R
20°
40°
Fig 9
t x 10-3 IN

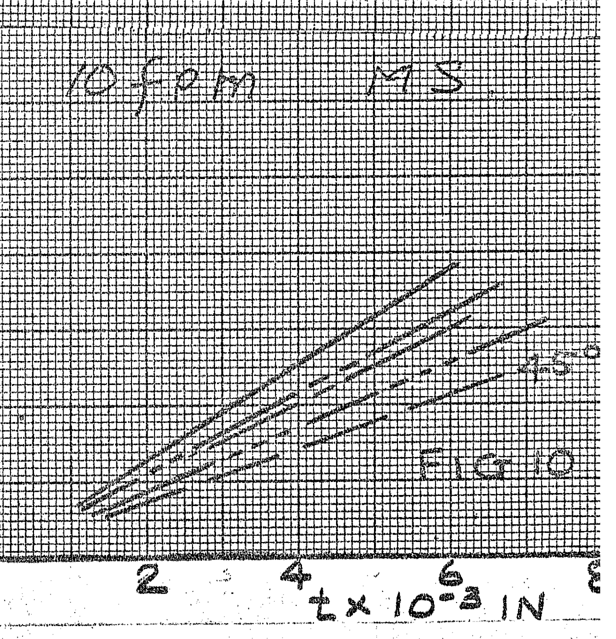
10 fpm
M S
R
45°
Fig 10
t x 10-3 IN

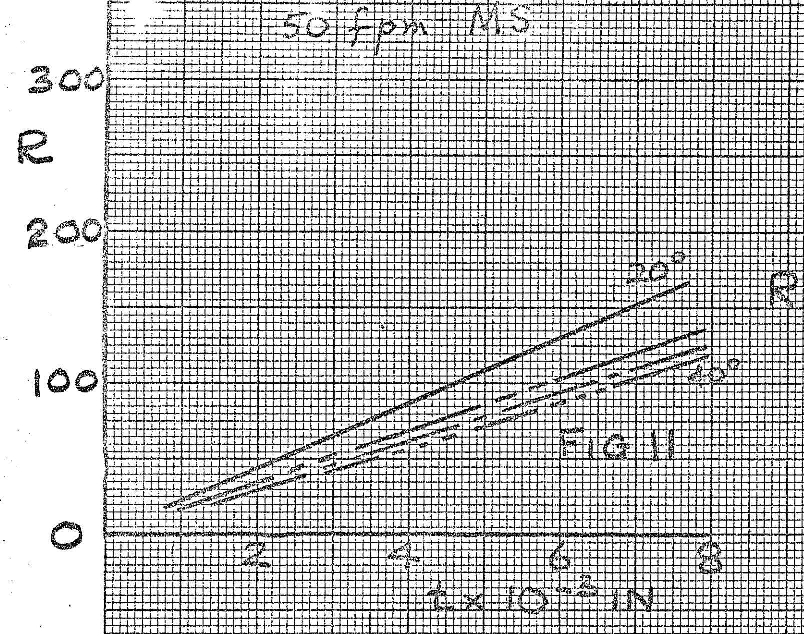

FIG 11

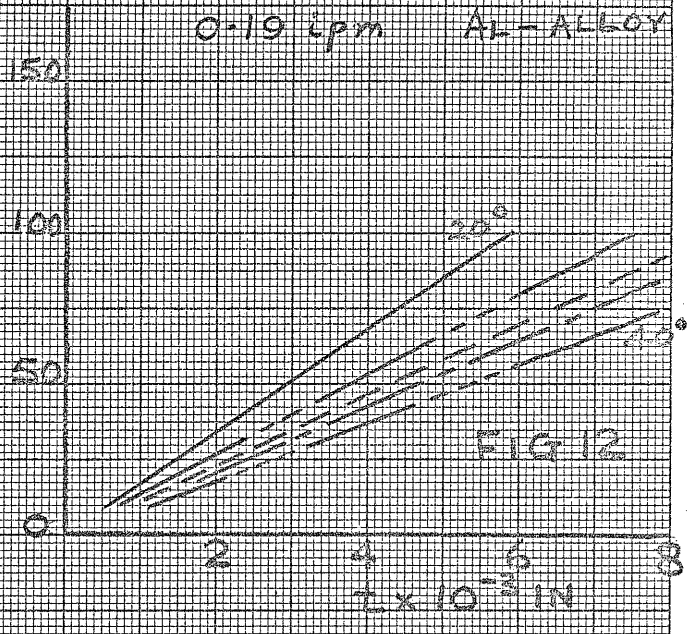

FIG 12

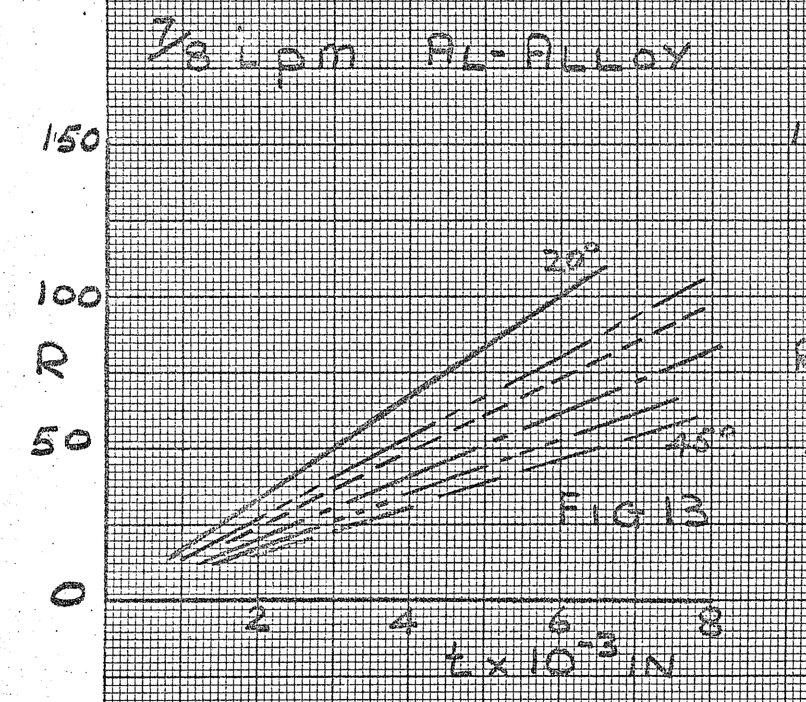

FIG 13

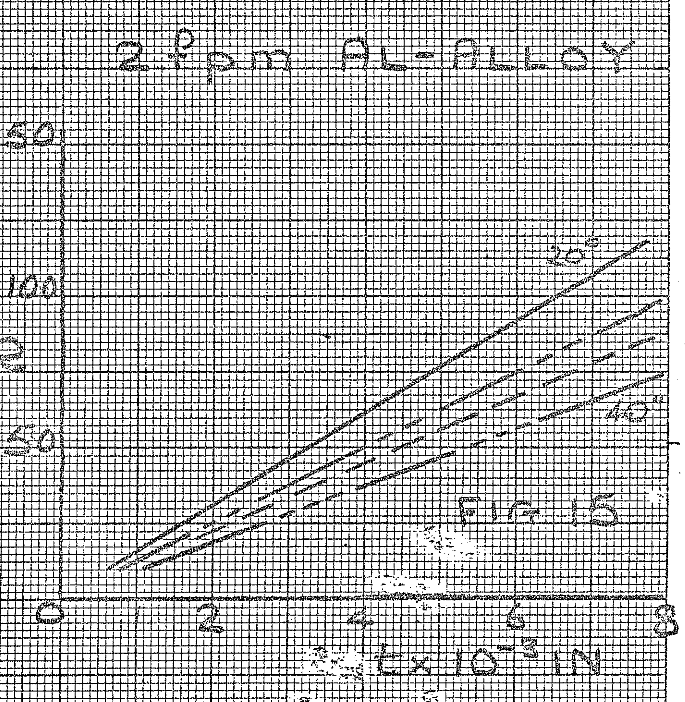

FIG 15

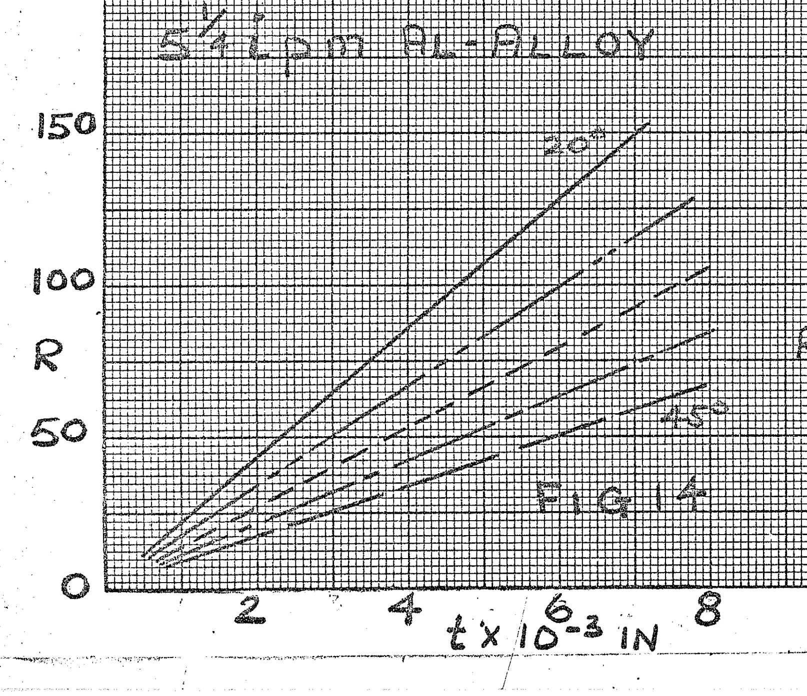

FIG 14

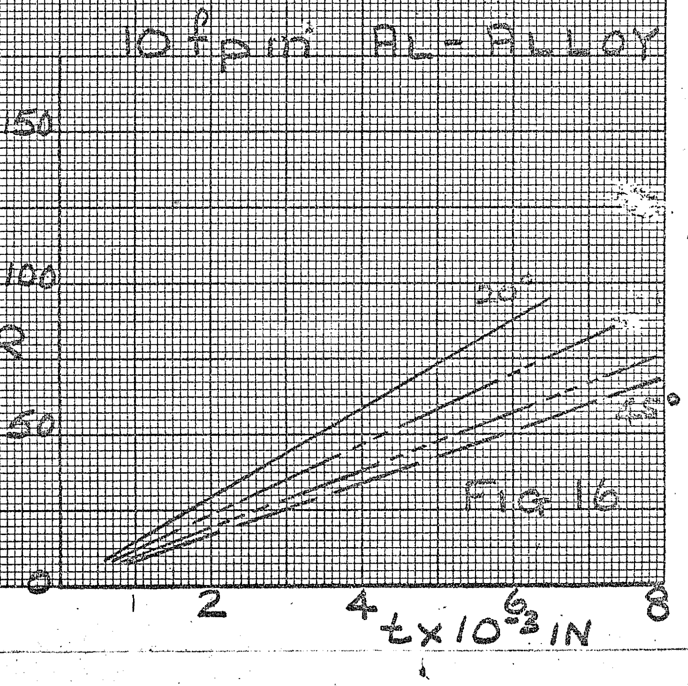

FIG 16

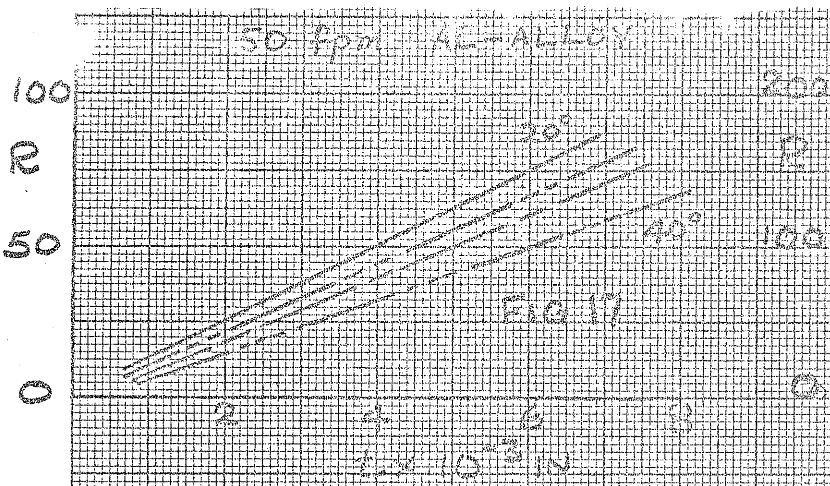
50 fpm AL-ALLOY
100
R
50
0
30°
40°
FIG 17
2
4
6
8
t x 10⁻³ IN

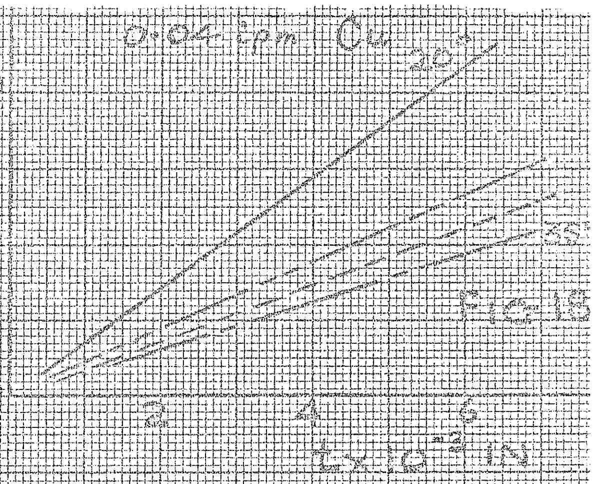
0·04 fpm Cu
200
R
100
0
20°
FIG 18
2
4
6
t x 10⁻³ IN

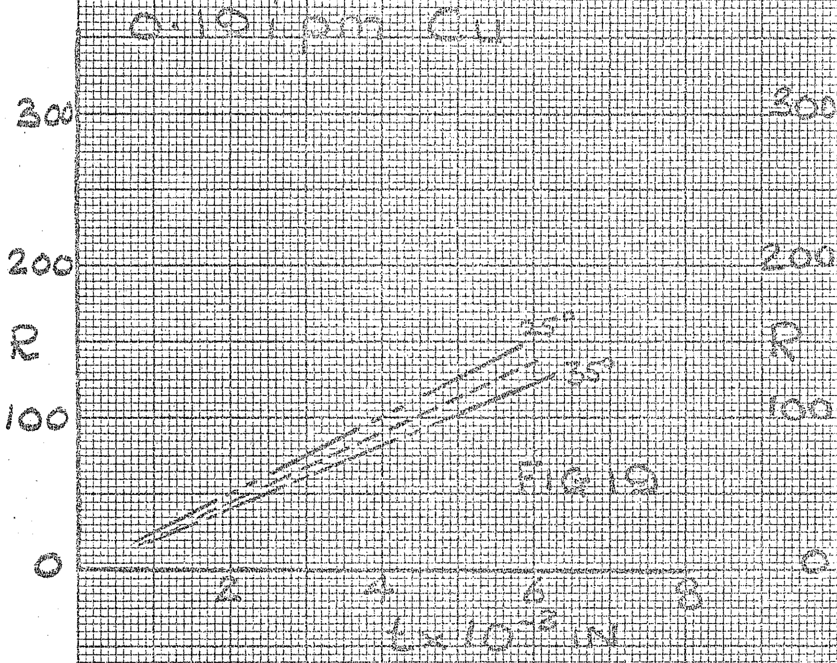
0·19 fpm Cu
300
200
R
100
0
25°
35°
FIG 19
2
4
6
8
t x 10⁻³ IN

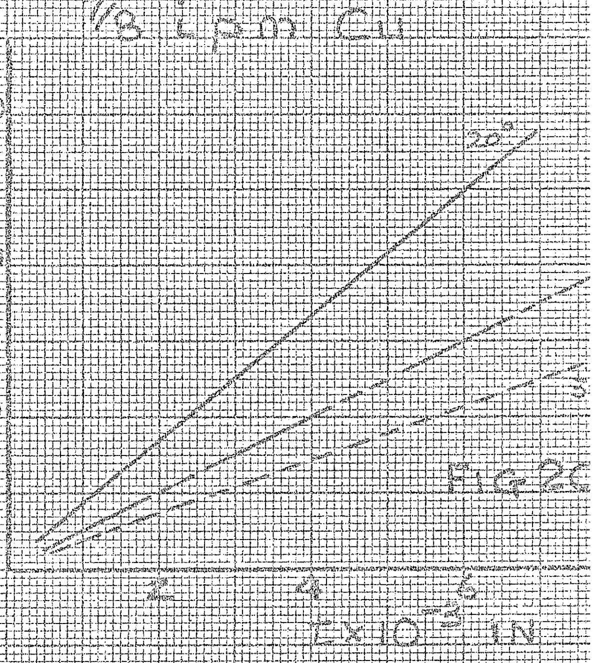
7/8 fpm Cu
300
200
R
100
0
20°
2
4
6
t x 10⁻³ IN

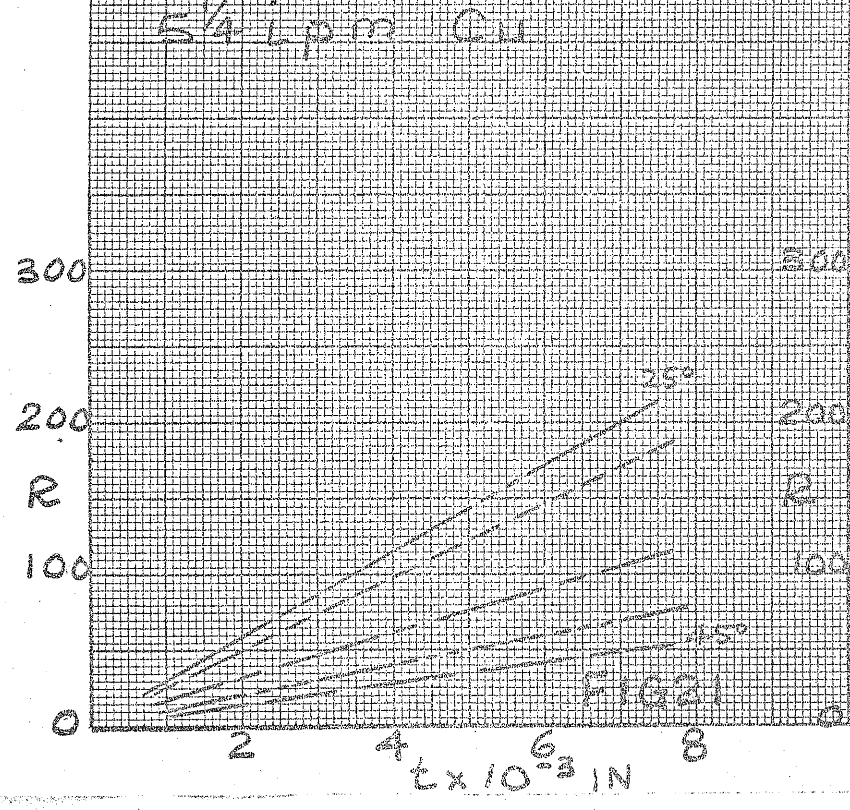
5¼ fpm Cu
300
200
R
100
0
25°
45°
FIG 21
2
4
6
8
t x 10⁻³ IN

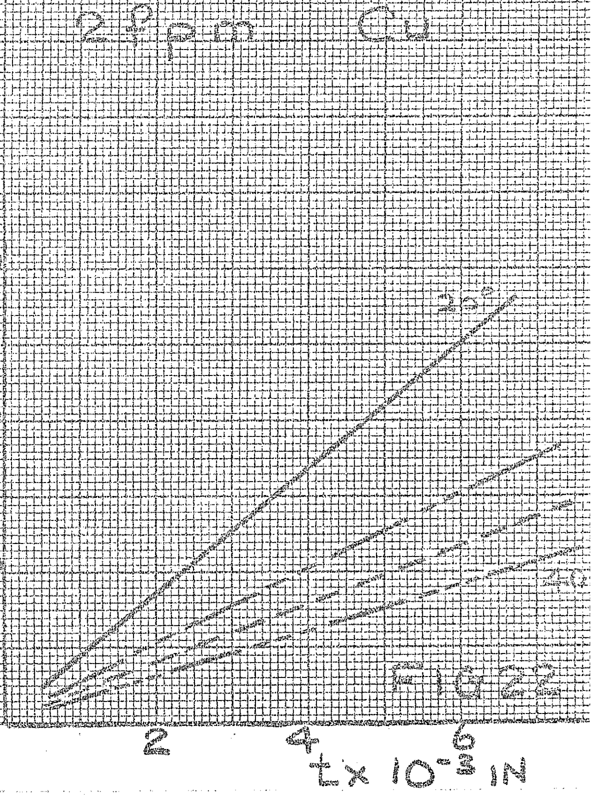
2 fpm Cu
300
200
R
100
0
20°
FIG 22
2
4
6
t x 10⁻³ IN

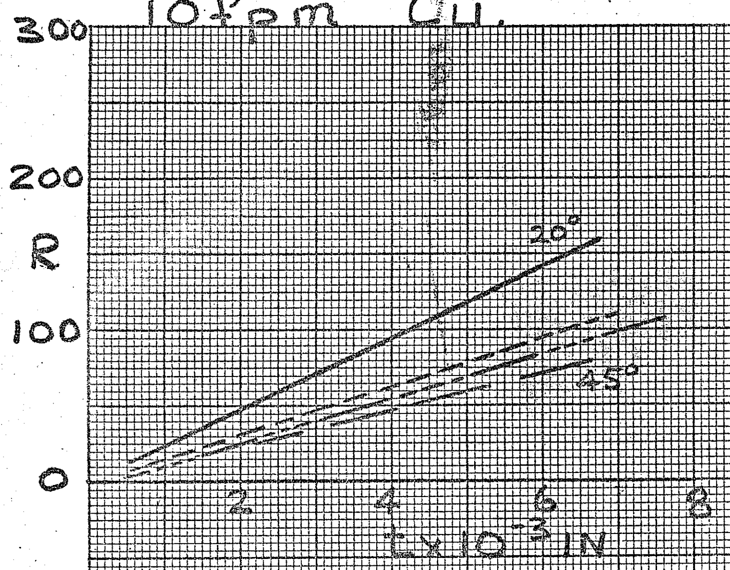
10 fpm Cu.
300
200
R
20°
100
45°
0
2
4
6
8
t x 10^{-3} IN

FIG.23

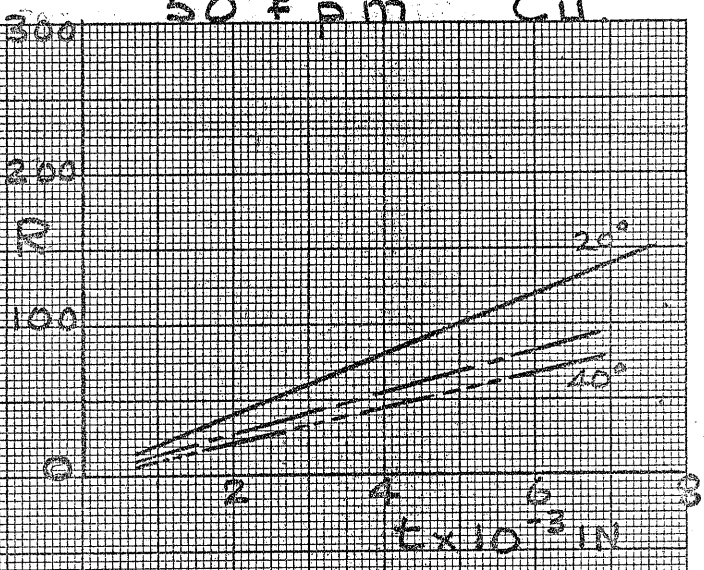
50 fpm Cu.
300
200
R
20°
100
40°
0
2
4
6
8
t x 10^{-3} IN

FIG 24

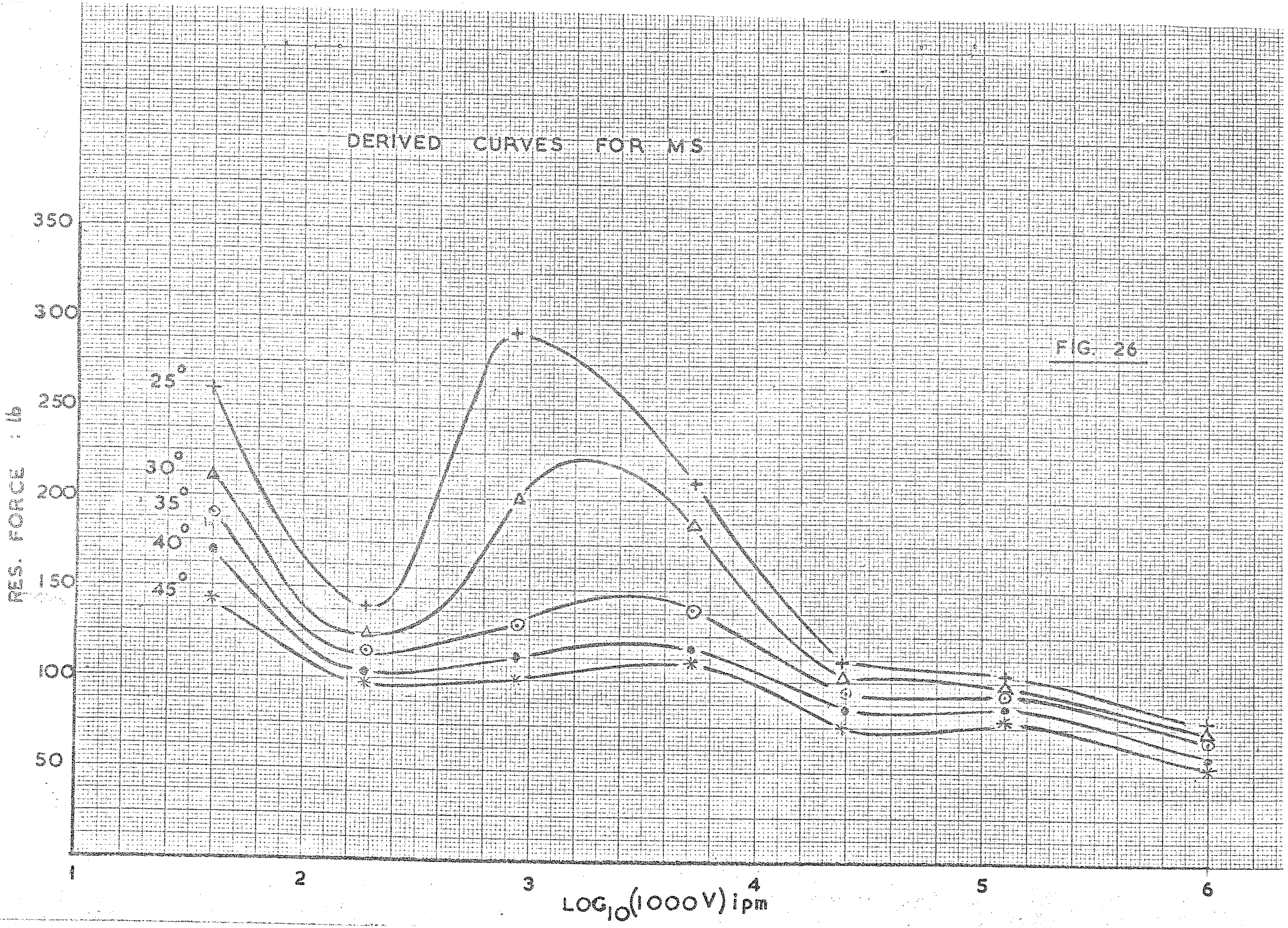

DERIVED CURVES FOR MS
RES. FORCE : lb
350
300
250
200
150
100
50
25°
30°
35°
40°
45°
1
2
3
4
5
6
LOG$_{10}$(1000V) ipm

FIG. 26

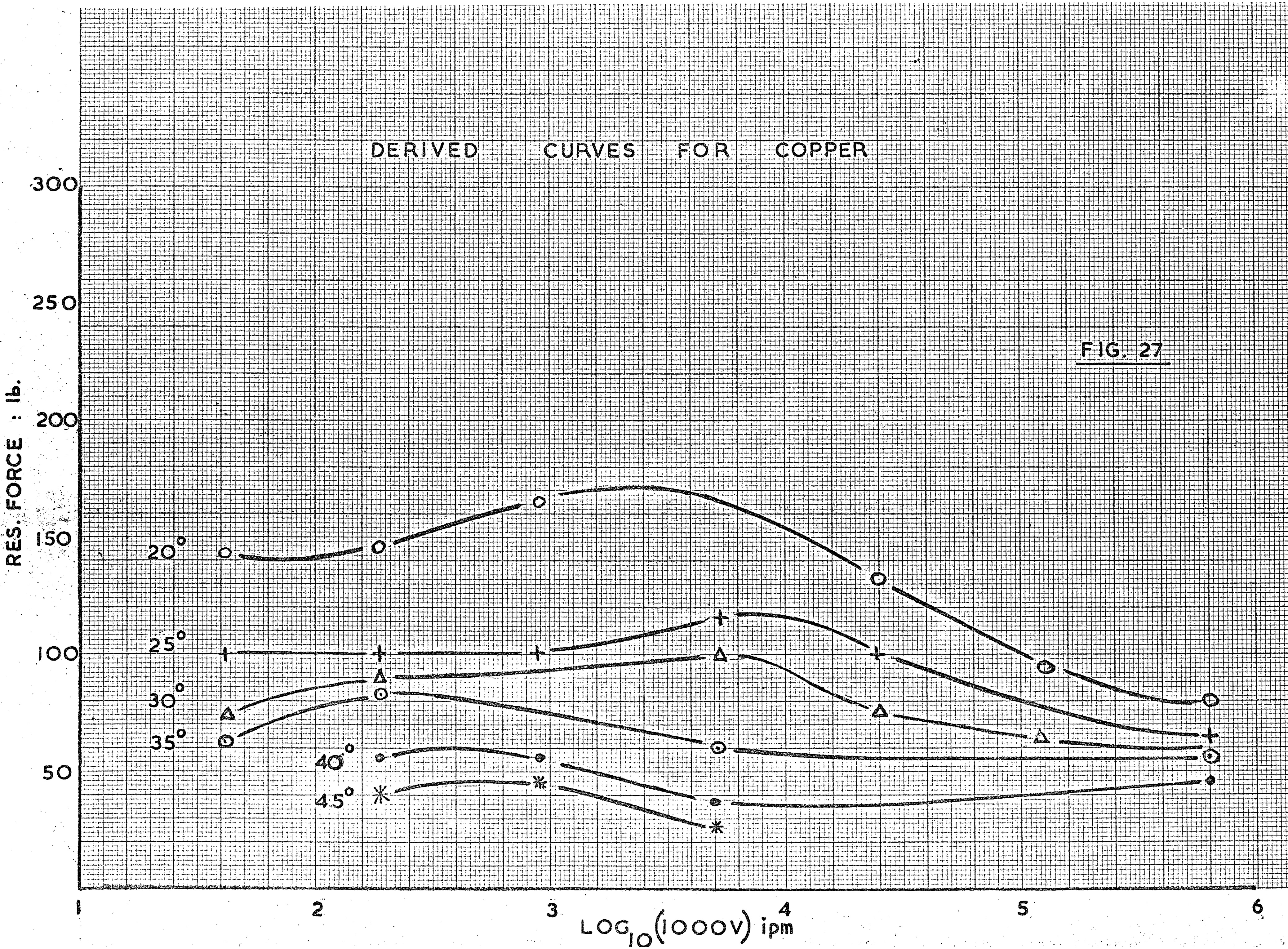
DERIVED CURVES FOR COPPER
RES. FORCE : lb.
300
250
200
150
100
50
20°
25°
30°
35°
40°
45°
1
2
3
4
5
6
LOG$_{10}$(1000V) ipm

FIG. 27

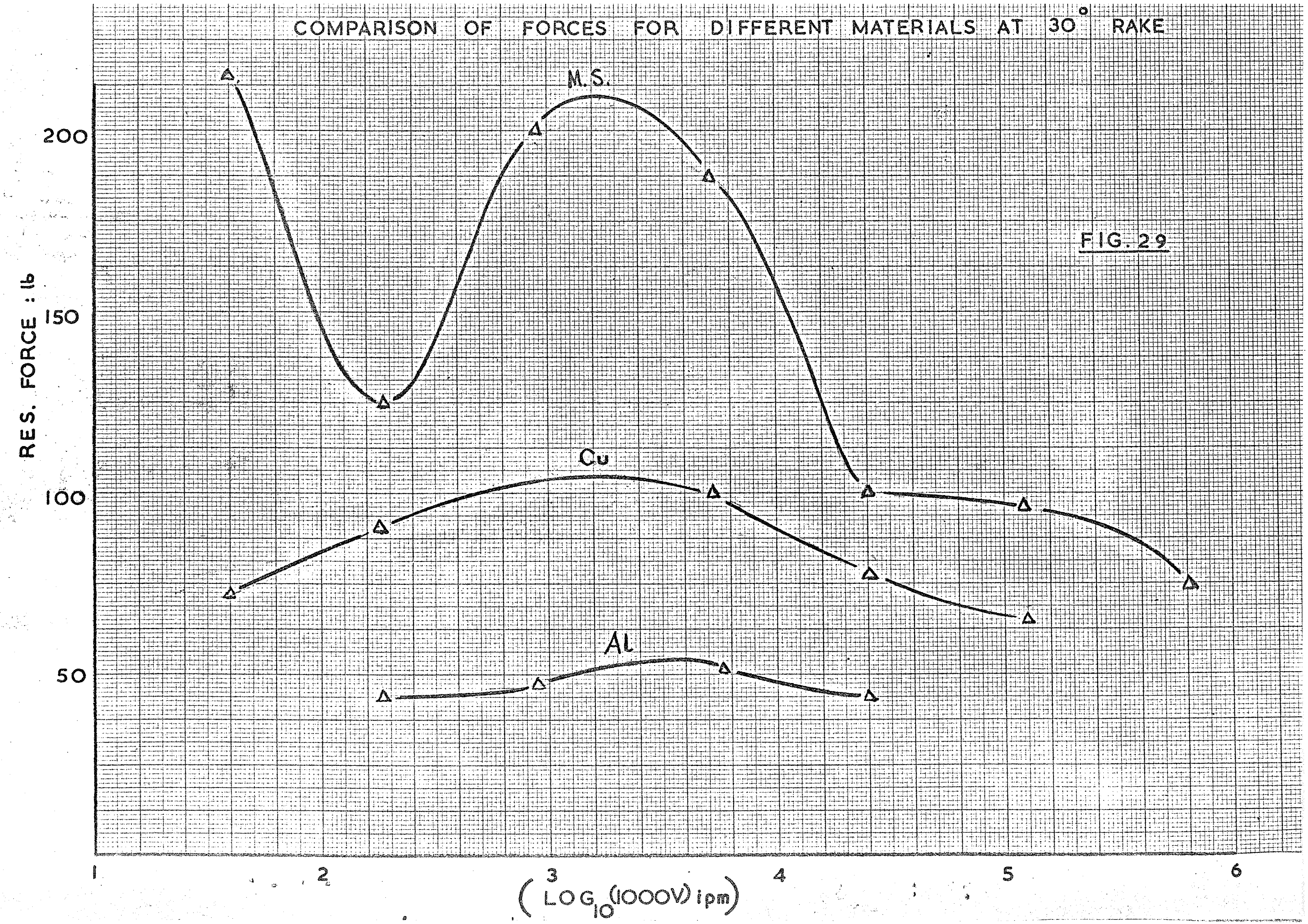

COMPARISON OF FORCES FOR DIFFERENT MATERIALS AT 30° RAKE
M.S.
Cu
Al
FIG. 29
RES. FORCE : lb
200
150
100
50
1
2
3
4
5
6
(LOG10(1000V) ipm)

DERIVED CURVES FOR ALUMINIUM

FIG. 28

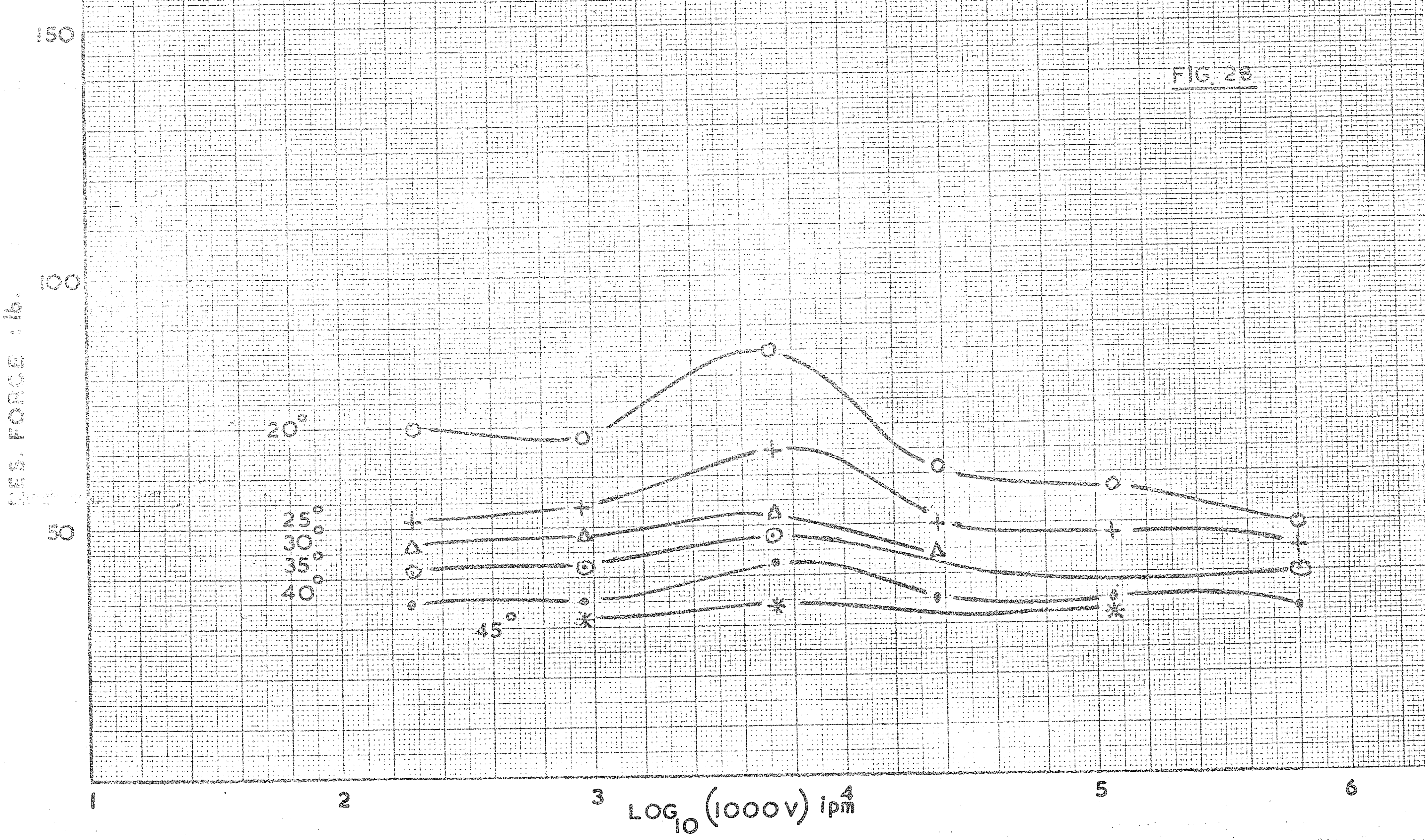

FIG. 32

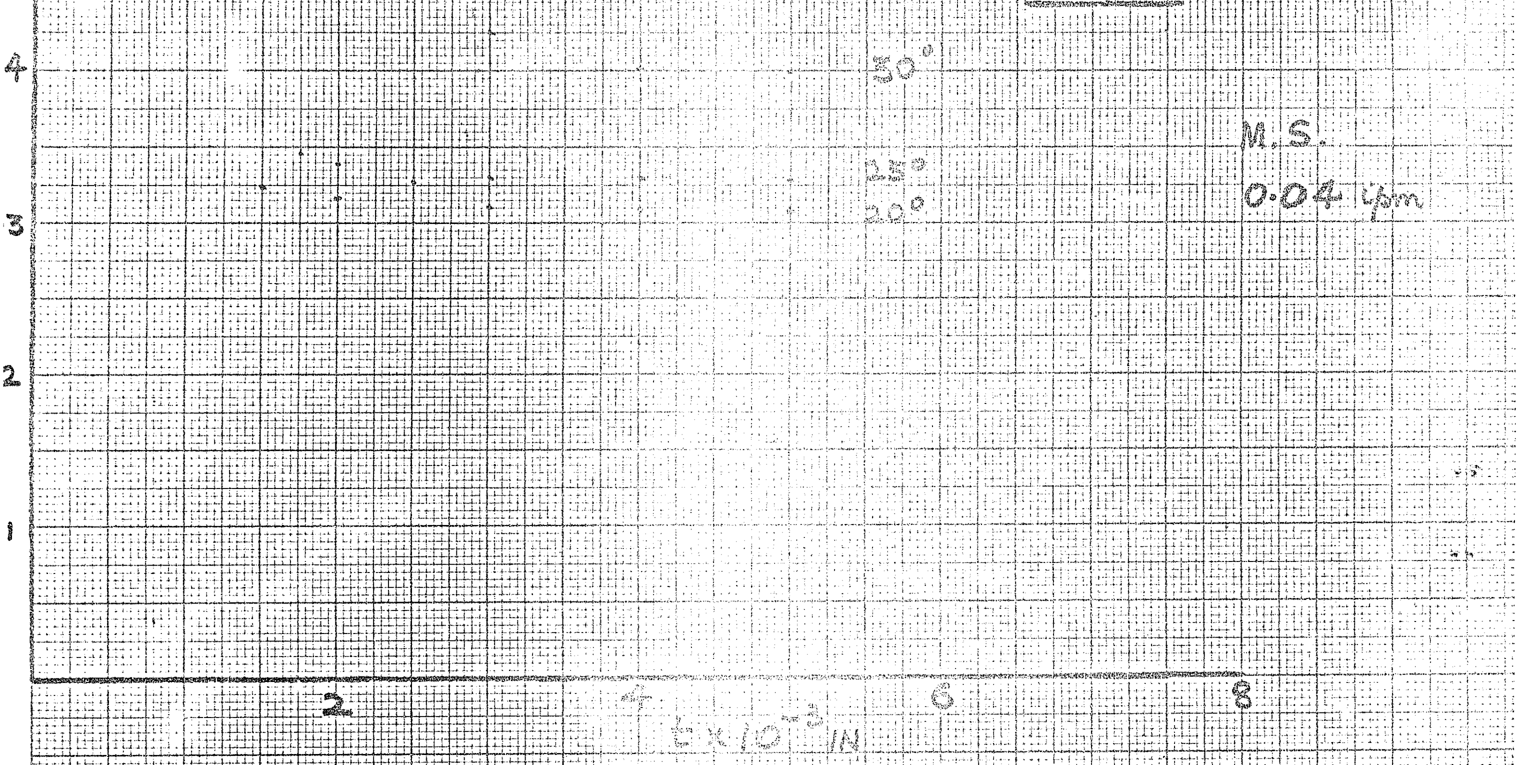
30°
25°
20°
M.S.
0·04 ipm
4
3
2
1
2
4
6
8
ε x 10^-3 IN

FIG. 33

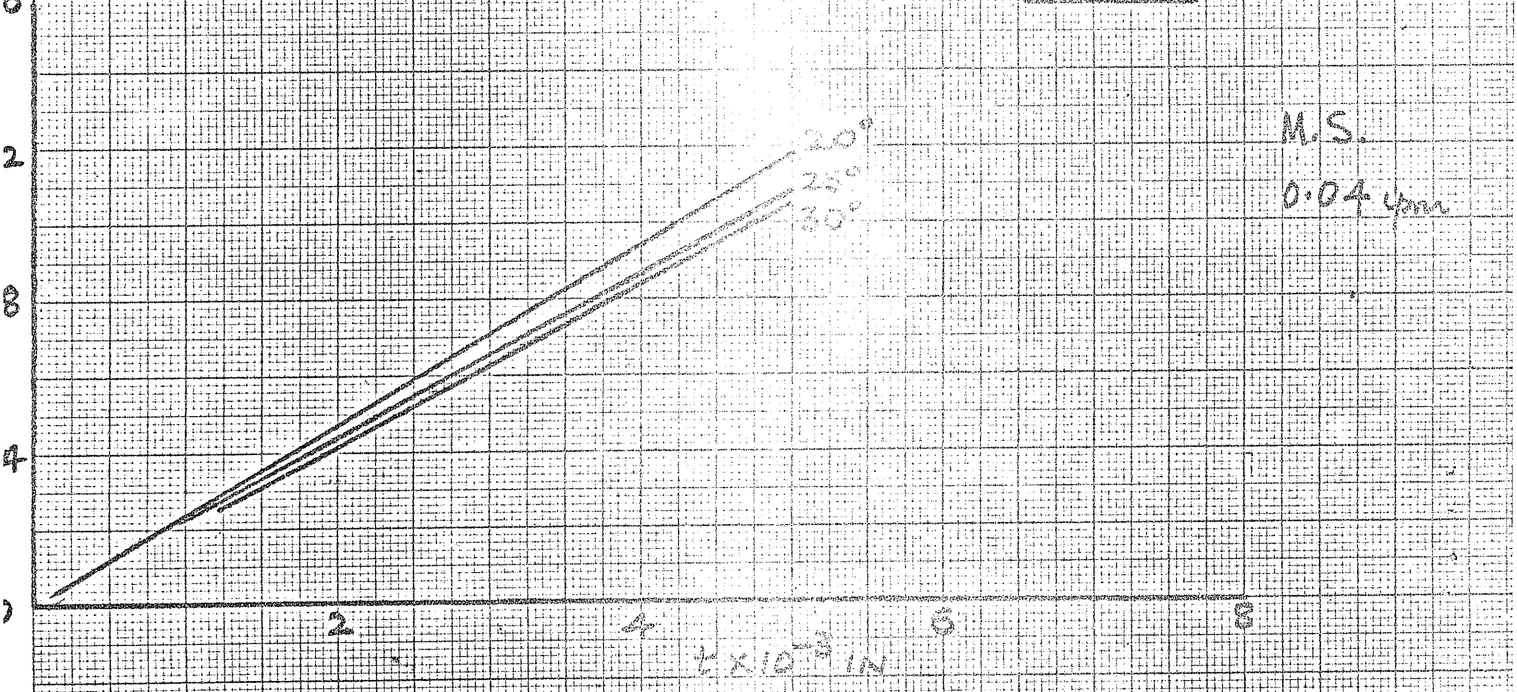
20°
25°
30°
M.S.
0·04 ipm
6
2
8
4
2
4
6
8
ε x 10^-3 IN

FIG. 30

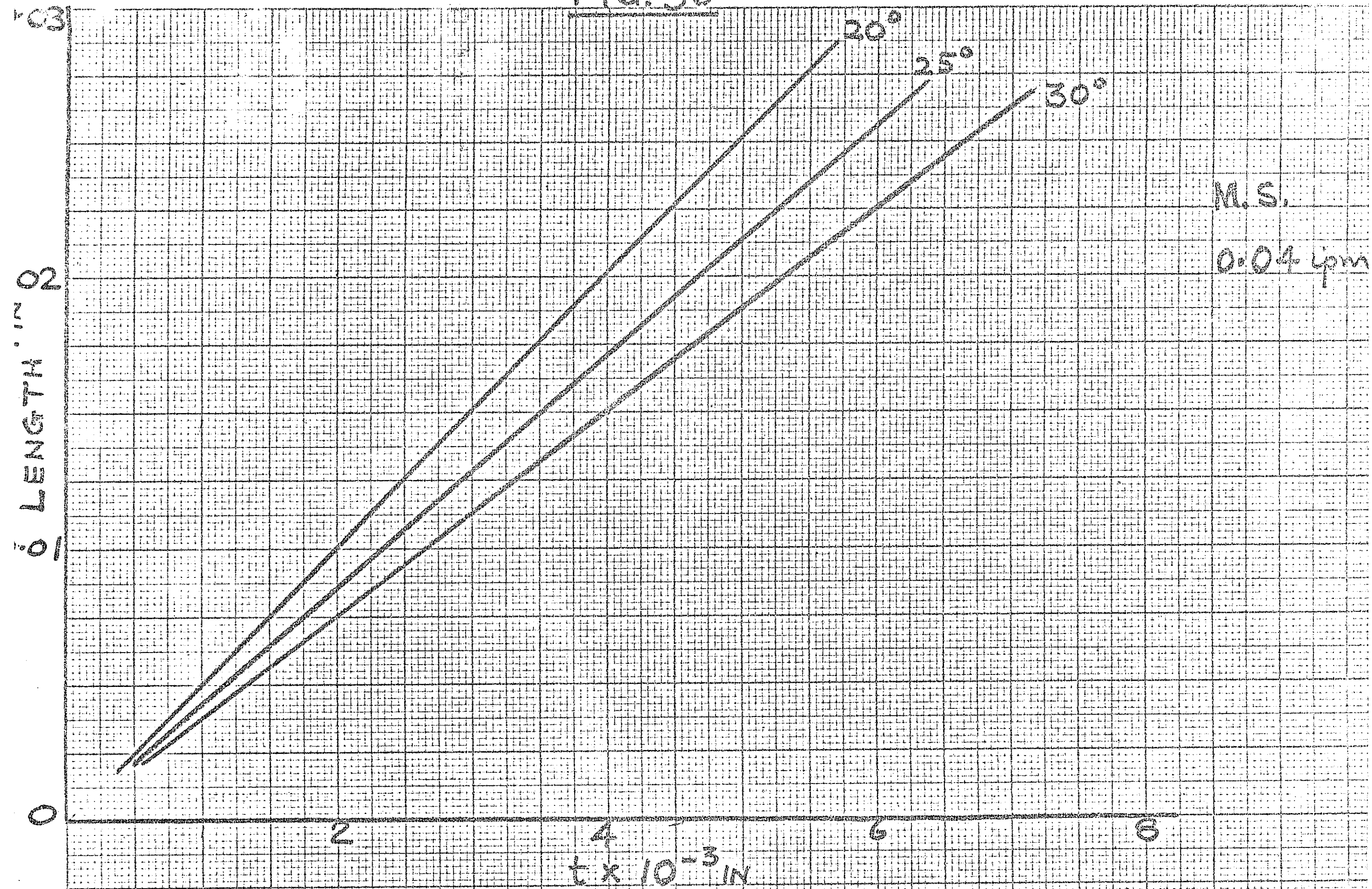

20°
25°
30°
M.S.
0.04 ipm
·03
·02
·01
0
δ LENGTH IN
2
4
6
8
t x 10⁻³ IN

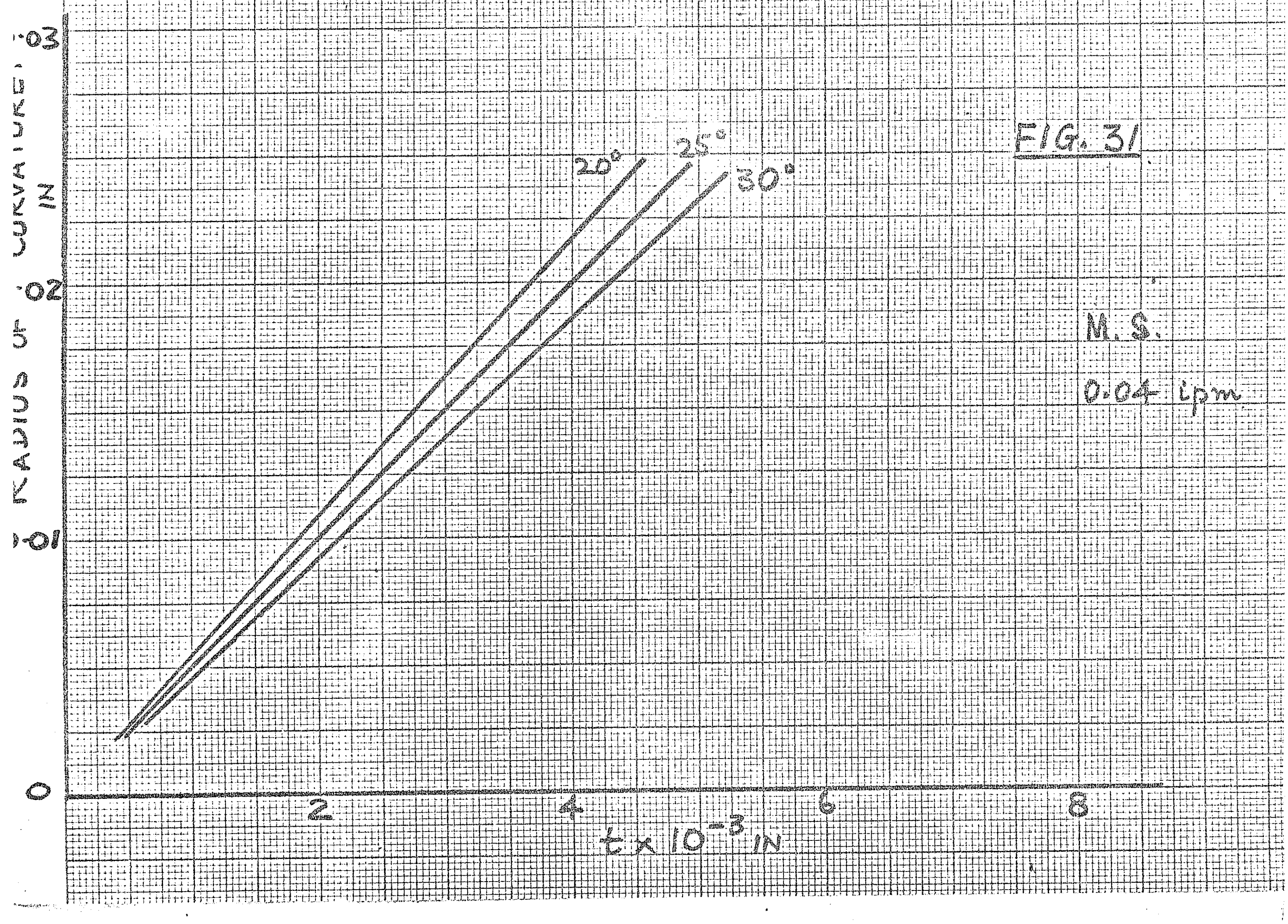

20°
25°
30°
M.S.
0.04 ipm
·03
·02
·01
0
RADIUS OF CURVATURE IN
2
4
6
8
t x 10⁻³ IN

FIG. 31